Proceedings of the 6th Nordic Signal Processing Symposium - NORSIG 2004
June 9 - 11, 2004
Espoo, Finland

Bone Segmentation WA-algorithm

Dusan Heric[†], *Bozidar Potocnik*

University of Maribor
Faculty of Electrical Engineering and Computer Science
System Software Laboratory
Smetanova 17, 2000 Maribor, Slovenia

[†]E-mail: dusan.heric@uni-mb.si

ABSTRACT

This article introduces a new bone segmentation WA-algorithm in the MR images. The algorithm is based on the wavelet and the active contour theory. It is semi-automatic. An expert has to select a starting point in region of interest. Algorithm's execution could be roughly separated into two steps. First the edge enhancement is performed which is done with wavelet transform and, a candidate points' extraction. In the second step followed by the fine detection of bone's boundary is performed with the active contours theory.

The proposed WA-algorithm quality and reliable segments bones on testing MR-images of knee-joint. In general this algorithm is able to quality segment the bones on any MR-image, which are same modality as testing images.

1. INTRODUCTION

The discoveries of X-rays, ultrasound and magnetic resonance, have brought up to the rapid development of medical imaging technologies. Those technologies allow scientists and physicians to obtain potentially live-saving information by peering harmless into the human body. Gradually, the role of medical imaging assistance has expanded beyond the simple visualization and inspection of anatomical structures. Beside that, they have become assistance for surgical planning.

Nowadays, medical imaging is playing a prominent role in the diagnosis and treatment of diseases. The need for extracting clinically useful information is obvious [2, 3]. Consequently the main challenge is to construct quality, reliable, fast and accurate segmentation algorithm for particular domain. Therefore many different segmentation approaches has been proposed in [4, 5].

We dealt with detection of bone boundary in the MR-images. The main disadvantage of such images is weak bone boundary, texture over bone and image intensity inhomogeneity. Beside that, we are confronted with the problem of ground truth, because absolutely ground truth of medical images does not exist (presence of different artefacts, noise, inter-intra observer variability, etc.). Therefore we tested the WA-algorithm's accuracy on the synthetic and medical MR-images.

2. FORMULATION

The mathematical foundation of WA-algorithm represents the confluence of wavelet and active contours theory. Wavelet transform serves to enhance the object boundary, while active contour imposes constraint on how the contour vary over space and time.

2.1 Wavelet basis

The wavelet transform maps a time function *s(t)* into a two-dimensional function with two independent parameters α and τ. The parameter α is scale and τ is the translation of the wavelet function along the time axis. The continuous wavelet transform of signal *s(t)* is [7]

$$CWT(\alpha,\tau) = \frac{1}{\sqrt{a}} \int s(t)\psi\left(\frac{t-\tau}{a}\right)dt, \qquad (1)$$

where ψ is the basic wavelet.

In this work used is a basic wavelet *ψ(t),* a quadratic spline proposed in [8]. The quadratic spline Fourier transform is

$$\psi(\omega) = j\omega\left(\frac{\sin(\omega/4)}{\omega/4}\right)^4. \qquad (2)$$

Regarding our WA-algorithm, we are interested in enhancing the bone boundary. This wavelet was already applied to ECG signals in [9]. Because of similarity between ECG signals (QRT complex) and edges in our images, and comprehensive usage of such a type of basic wavelet in detecting ECG waves [9,10] we decided to use a same type of basic wavelets for the bone image enhancement.

For computational purpose we used algorithm called *algorithme à trous* [11], where signal representation is time-invariant. The scale parameter α is discretized and

follows a dyadic grid in the time-scale plane, thus $\alpha=2^k$. Such transform is called a dyadic wavelet transform [8]. Using this algorithm, the equivalent frequency response for the *k*-th scale is

$$Q_k(e^{j\omega}) = \begin{Bmatrix} G(e^{j\omega}) & k=1 \\ G(e^{j2^{k-1}\omega})\prod_{l=0}^{k-2} H(e^{j2^l\omega}) & k \geq 2 \end{Bmatrix}, \quad (3)$$

where the frequency parts *H* and *G*, with respect to basic wavelet $\psi(t)$, are

$$\begin{aligned} H(e^{j\omega}) &= e^{j\omega/2}(\cos\frac{\omega}{2})^3 \\ G(e^{j\omega}) &= 4e^{-j\omega/2}(\sin\frac{\omega}{2}) \end{aligned}. \quad (4)$$

The applied dyadic wavelet transform is similar to a fast biorthogonal wavelet transform, without subsampling [8].

2.2 Active Contours

Active contour were originally proposed by Kass [1] as a technique of matching a deformable model to a region boundary by energy minimization. The original active contours are elastic curves or splines defined in an image domain and have a dynamic behavior that evolves from an initial position in the image to converge to the object boundary. The initial position is provided either by interactive action of the user of by a higher-level process [1].

The active contours are time dependent planar deformable curves, written in parametric form

$$v(s,t) = (x(s,t), y(s,t)), \quad (5)$$

where *x* and *y* are curve's coordinate at time *t*. The variable *s* is proportional to the arc length, $s \in [0,1]$. The active contour changes its position in time according to the minimization of the energy functional *E*

$$E(v(t)) = \int_0^1 E_{\text{int}}(v(s,t))ds + \int_0^1 E_{ext}(v(s,t))ds = \frac{1}{2}\int_0^1 (\alpha(s)\left|\frac{\partial v(s,t)}{\partial s}\right|^2 + \beta(s)\left|\frac{\partial^2 v(s,t)}{\partial s^2}\right|^2)ds + \int_0^1 P(v(s,t))ds, \quad (6)$$

where E_{int} represents internal energy of the active contour, α and β are arbitrary functions, which regulate the curve's tension and rigidity. *P(v)* is a scalar potential function defined over the image plane and which is typically computed through image intensity. The local minima of *P(v)* could be interpreted as active contour attractors.

The deformation process of the active contour is driven by minimization of the energy functional (6). An active contour that minimizes the energy functional (6) must satisfy the Euler equation [1]

$$\frac{\partial}{\partial t}v(s,t) = \frac{\partial}{\partial s}\left(\alpha\frac{\partial v}{\partial s}(s,t)\right) - \frac{\partial^2}{\partial s^2}\left(\beta\frac{\partial^2}{\partial s^2}v(s,t)\right) - \nabla P(v(s,t)). \quad (7)$$

The equation (7) can be also interpreted as a force balance, where energies are associated with the forces [12]

$$F_{\text{int}} + F_{ext} = 0, \quad (8)$$

where F_{int} and F_{ext} denote the internal and external forces as

$$\begin{aligned} F_{\text{int}} &= \frac{\partial}{\partial s}\left(\alpha\frac{\partial v}{\partial s}(s,t)\right) - \frac{\partial^2}{\partial s^2}\left(\beta\frac{\partial^2}{\partial s^2}v(s,t)\right) \\ F_{ext} &= -\nabla P(v(s,t)) \end{aligned}. \quad (9)$$

While the internal force is responsible for preserving the shape of the active contour, the external force drives the active contour to the boundary. The external force is primarily the image force, computed based on the image itself, and a constraint force can optionally be added. WA-algorithm uses the Gradient Vector Flow (GVF) as image force proposed in [12].

The deformation process stops when forces are balanced. The actual position of the snake is calculated by iterating through the numerical equation (10).

$$\begin{aligned} x_t &= (A+\gamma I)^{-1}(\gamma x_{t-1} - f_x(x_{t-1}, y_{t-1})) \\ y_t &= (A+\gamma I)^{-1}(\gamma y_{t-1} - f_y(x_{t-1}, y_{t-1})) \end{aligned}, \quad (10)$$

where the matrix $A+\gamma I$ is a pentadiagonal banded matrix and γ defines the viscosity parameter [1]. Parameters $f_x = \partial E_{ext}/\partial x$ and $f_y = \partial E_{ext}/\partial y$ are approximated by a finite difference. That is derived form the equation (7) and its minimization procedure are given in [1].

3. WA-ALGORITHM

The WA-algorithm structure is standard by following the ideas presented in [4, 6]. It is generic, semi-automatic and is specially designed for bone's boundary detection in

MR-images. Algorithm inputs into the are image I and starting point $p(x,y)$. The starting point p has to lie in the region of interest.

The algorithm's execution is divided into four steps: a) cartesian to polar coordinate transformation, b) edge enhancement, c) detection of boundary candidate points, and d) fine tuning of object's boundary.

Cartesian to polar coordinate transformation is the first stage in the algorithms' execution chain. The starting point p is an origin of the polar coordinate system. The transformation maps straight lines between the point p and all image border points to polar coordinates (Fig. 1).

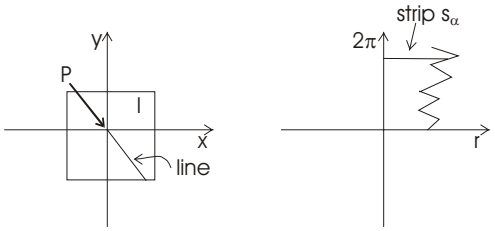

Fig. 1. Cartesian to polar coordinate transformation.

Transformation results are in a new image I', which is actually a set of strips or vectors s_α. The discrete parameter α is calculated in mapping process and denotes the angle between 0 and 2π. In this way, the image I is decomposed into the set of one-dimensional vectors. These vectors are in next stage transformed by using wavelet transform with wavelet (2). Fig. 2 depicts an example of arbitrary vector s_α and its wavelet transform.

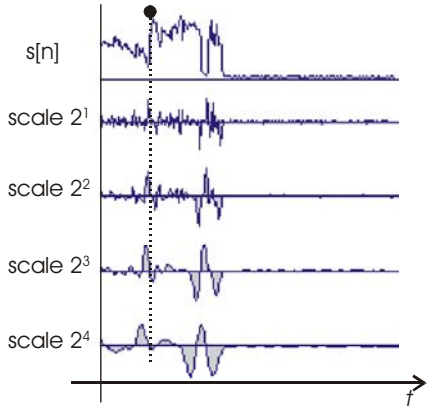

Fig. 2. Wavelet transform at first four scales of arbitrary vector from our MR-images.

Black circle (see Fig. 2.) denotes an actual object edge point annotated by an expert. Through the earlier analysing process it was discovered that the bone edges and their corresponding signal s_α represent as a increasing function from low to high value, and finished by small decline. Such wave is after the wavelet transformation indicated as a zero crossing between two slopes, where one of them is significant.

The wavelet transform is followed by the stage of candidate points' extraction. From the frequency responses of the wavelet (2) at scales 2^k in [8] $(k=1,...,6)$ and a spectrum of edge wave in our arbitrary signal (see Fig. 3.), it is clear that most of signal energy of the edge lies within the scale 2^k $(k=1,...,4)$. For scales higher than 2^4 the energy of edge is very low. We decided to pick up the candidate point from the transformed strip at scale 2^2 marked as ts_a, which passes frequencies between 0 and 90 Hz.

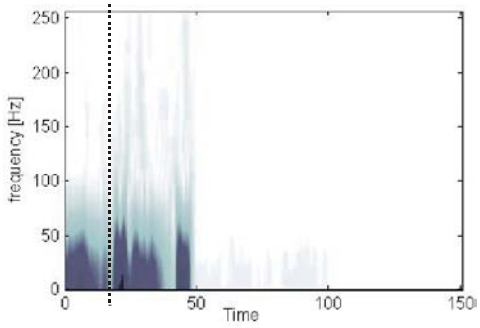

Fig. 3. The dotted straight line denotes the spectrum of edge point in our MR image.

The process of denoting the particular point as candidate edge point is adaptive. This selection respects two criteria. First with thresholding technique, all possible edge points as selected. The second condition is sliding standard deviation of candidate points. Sliding standard deviation is standard deviation over candidate points on limited angle interval. It picks up one candidate point from each strip and combines it with other candidate points from neighbouring strips. In special case in which candidate points at specific angle do not exist, the strip s_α is ignored.

Threshold is calculated as a mean value of vector ts_a.

$$T = \mu(ts_a[n]) . \tag{11}$$

The result of thresholding over ts_a is strip x_α. Finally, among edge points in x_α, a group of points with minima sliding standard deviation on interval $[0, 2\pi]$ is selected, Width of sliding window is $\pi/100$. The result of edge point extractions is set of object's edge points. In this way is only one candidate point selected from the vector $s[n]$.

The final step in segmentation procedure is fine object's boundary tuning. The candidate points are translated into cartesian coordinates. They present starting points for the active contour. Afterwards the input image is convoluted with Sobel edge detector. From the edge image the GVF is calculated. The parameters α and β are 0.5 and γ is 1. Finally the process of force balancing from (8) is executed. The WA-algorithm results in annotated object.

4. RESULTS

A set of tests was performed to check the efficiency and accuracy of bone segmentation WA-algorithm. High-quality static MR-images of dimensions 512x512pixels, acquired with T1 weight, through human knee joint were used. An effective pixel size was around 0.4 mm. The WA-algorithm performance was evaluated with four statistical measures: ratios *r1*, *r2*, *Hausdorff distance–HD* and *Mean Absolute Distance–MAD* presented in work [13]. As the reference annotations were used manually annotated objects by the expert.

Fig. 4 depicts the annotated bone tibia in MR image. The left image presents the ground truth of the bone tibia, while the second one depicts segmentation result. From the physician point of view the most important and interesting region of knee-joint is marked with dotted white circle in Fig. 4(a). Therefore, the accuracy of WA-algorithm was calculated only inside this area.

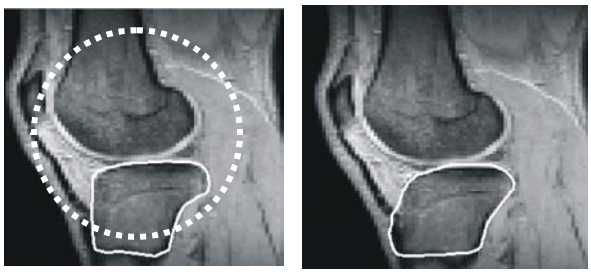

Fig. 4. An instance of annotated bone tibia in MR image; a) manually annotated bone tibia by expert, b) WA-algorithm result.

The tests were performed on 9 medical images. Table 1 depicts the average statistical parameters for bones femur and tibia.

Table 1. The average statistical parameters for bones femur and tibia.

Bone	r1 [%]	r2 [%]	MAD [mm]	HD [mm]	Time [s]
Femur	0.97	0.91	0.99	3.13	6.2
Tibia	0.91	0.92	1.25	4.17	6.4

The average distance between the reference and computer detected border is about 1 mm. The ratios *r1* and *r2* confirm a good match between computer and experts regions. Hausdorff distance measures the biggest error between two curves and it is usually high. In addition, the time consumption to determinate observed object is low and constant, about 6 seconds. Therefore, the algorithm could be used in an interactive bone segmentation tool.

5. CONCLUSION

The proposed algorithm precisely detects the bone structures in MR-images. It could also be applied to the images with similar characteristics of regions boundaries. Only limitation is the algorithm's incapability to segment very convex regions. Regardless of this weakness the algorithm originally was designed as a bone segmentation algorithm.

ACKNOWLEDGMENT

The authors gratefully acknowledge the indispensable contribution of Dr. Tomaz Tomazic from the Teaching Hospital of Maribor, Slovenia, whose manual annotations of the MR recordings enabled verification of this research.

REFERENCES

[1] M. Kass et.al. "Snakes: Active Contour Models," *International Journal of Computer Vision*, vol. 1 pp. 321-331, 1987.
[2] N. Ayache, "Medical computer vision, virtual reality and robotics" *Image and Vision Compution* vol, 13. ed. 4 pp. 195-313, 1995.
[3] W. Wells, A. Colchester, and S. Delp, Eds. "Medical Image Computing and Computer-Assisted Intervention" *Proc. 1st Int. Conf. (MICCAI'98)*, Cambridge, MA, USA, October, 1998, volume 1496 of Lecture Notes in Computer Science.
[4] I. N. Bankman, Handbook of Medical Imaging Processing and Analysis, *Academic Press*, 2000.
[5] J. R. Parker, Algorithms for Image Processing and computer Vision, John Wiley & Sons, Inc. 1997.
[6] M. Akay, Time Frequency and Wavelets in Biomedical Signal Processing, IEEE Press, 1998.
[7] Y. T. Chan, Wavelet Basics, Kluwer Academic Publishers, 1995.
[8] S. Mallat, A Wavelet Tour of Signal Processing, Academic press, 1998.
[9] A. S. M. Koeleman, H. H. Ros, and T.J. van den Akker, "Beat-tobeat interval measurement in the electrocardiogram,"Med. Biol. Eng. Comput., vol. 23, pp. 213-219, 1985.
[10] M. Bahoura, M. Hassani, and M. Hubin, "DSP implementation of wavelet transform for real tiem ECG wave forms detection and heart rate analysis", Computer Methods and Programs in Biomedicine, no. 52, pp. 34-44, 1997.
[11] A. Cohen and J. Kovačević, "Wavelets: the mathematical background", Proceedings of the IEEE, vol. 84, no. 4, pp. 514-522 1996.
[12] C. Xu, J.L. Prince, "Gradient vector flow: a new external force for snakes," *Proc. IEEE Conf. on Computer Vision and Pattern Recognition*, pp. 66-71, 1997.
[13] SimBio Consortium, "SimBio-A Generic Environment for Bio-numerical Simulation", http://www:simbio:de/~simbio/.